Stunted children display ectopic small intestinal colonization by oral bacteria, which cause lipid malabsorption in experimental models

Pascale Vonaesch[a,b,c,d,e,2], João R. Araújo[a,b,3], Jean-Chrysostome Gody[f], Jean-Robert Mbecko[g], Hugues Sanke[g], Lova Andrianonimiadana[h,1], Tanteliniaina Naharimanananirina[i], Synthia Nazita Ningatoloum[f], Sonia Sandrine Vondo[f], Privat Bolmbaye Gondje[f], Andre Rodriguez-Pozo[a,b,j], Maheninasy Rakotondrainipiana[k], Kaleb Jephté Estimé Kandou[l], Alison Nestoret[m], Nathalie Kapel[m], Serge Ghislain Djorie[l], B. Brett Finlay[n], Laura Wegener Parfrey[o], Jean-Marc Collard[f,4], Rindra Vatosoa Randremanana[k], Philippe J. Sansonetti[a,b,2,4] (ID), and The Afribiota Investigators[5]

Environmental enteric dysfunction (EED) is an inflammatory syndrome postulated to contribute to stunted child growth and to be associated with intestinal dysbiosis and nutrient malabsorption. However, the small intestinal contributions to EED remain poorly understood. This study aimed to assess changes in the proximal and distal intestinal microbiota in the context of stunting and EED and to test for a causal role of these bacterial isolates in the underlying pathophysiology. We performed a cross-sectional study in two African countries recruiting roughly 1,000 children aged 2 to 5 years and assessed the microbiota in the stomach, duodenum, and feces. Upper gastrointestinal samples were obtained from stunted children and stratified according to stunting severity. Fecal samples were collected. We then investigated the role of clinical isolates in EED pathophysiology using tissue culture and animal models. We find that small intestinal bacterial overgrowth (SIBO) is extremely common (>80%) in stunted children. SIBO is frequently characterized by an overgrowth of oral bacteria, leading to increased permeability and inflammation and to replacement of classical small intestinal strains. These duodenal bacterial isolates decrease lipid absorption in both cultured enterocytes and mice, providing a mechanism by which they may exacerbate EED and stunting. Further, we find a specific fecal signature associated with the EED markers fecal calprotectin and alpha-antitrypsin. Our study shows a causal implication of ectopic colonization of oral bacterial isolated from the small intestine in nutrient malabsorption and gut leakiness in vitro. These findings have important therapeutic implications for modulating the microbiota through microbiota-targeted interventions.

environmental enteric dysfunction | stunted child growth | lipid malabsorption | low-grade inflammation | small intestine

Stunting is the most common form of childhood undernutrition, affecting roughly 142 million children globally. It has severe long-term effects, including cognitive delays, higher morbidity, and a higher risk of cardiovascular disease (1, 2). Nevertheless, to date, treatment strategies are limited, and even the best interventions can only correct for a fraction of the encountered growth delay and associated pathophysiological disturbances (3). In recent years, evidence has accumulated that the microbiota plays a crucial role in undernutrition in both its acute and chronic forms (4–6). Recently, we have shown that stunted children living in two different sub-Saharan African countries suffer from small intestinal bacterial overgrowth (SIBO) that is characterized by the presence of an excessive abundance of bacteria that normally reside in the oropharyngeal tract (7). These results have since been replicated in a study in Bangladesh, where the authors suggest that this bacterial signature is associated with small intestinal inflammation (8). Evidence has accumulated that a chronic inflammatory syndrome of the small intestine, called environmental enteric dysfunction (EED), plays a role in undernutrition (9). EED is characterized by an increase in the permeability of the small intestine and influx of immune cells into the gut epithelium, and it is thought to contribute to malnutrition via nutrient malabsorption (10).

Recent work in cell culture and mouse models suggests that members of the microbiota modulate dietary lipid digestion, absorption, storage, and secretion (11, 12). In this study, which is embedded in the Afribiota project (13), we aimed to characterize the small intestinal and fecal microbiota of children with stunting and/or EED and to assess for a causal role of the microbiota in the pathophysiology underlying stunted growth, especially intestinal inflammation and lipid absorption.

Significance

The intestinal microbiota and environmental enteric dysfunction (EED), an inflammatory syndrome of the small intestine, play a major role in chronic malnutrition. Nevertheless, the microbial changes remain little characterized. Here, we show that increased relative abundance of oral bacteria isolated from the small intestine is associated with reduced abundance of classical small intestinal bacteria. Experimental work further suggests the association of these small intestinal isolates with decreased lipid absorption and increased cell-layer permeability. Further, in the clinical study, we show that EED markers are associated with a decrease in butyrate-producing bacteria and an increase in *Fusobacterium* and *Megasphaera*. These findings pave the way for the development of microbiota-targeted interventions and thus, for better treatment of childhood undernutrition in the future.

[1]Deceased.

[2]To whom correspondence may be addressed. Email: pascale.vonaesch@unil.ch or philippe.sansonetti@pasteur.fr.

[3]Present address: NOVA Medical School, NOVA University of Lisbon, Lisbon, 1169-056 Portugal.

[4]Present address: The Center for Microbes, Development and Health, Chinese Academy of Sciences, Shanghai, 200031 China.

[5]A complete list of The Afribiota Investigators can be found in SI Appendix.

Results

Description of Study Population. After filtering out samples with low sequencing counts or that did not respect the inclusion criteria, we obtained fecal samples for 627 children, duodenal aspirates for 128 children, and gastric aspirates for 167 children, of which we had shared gastric and duodenal samples in 45 individuals, gastric and fecal samples in 218 individuals, and duodenal and fecal samples in 150 individuals. Fecal samples were available for moderately and severely stunted and nonstunted children, and duodenal samples were available for moderately and severely stunted children. The descriptions of the three cohorts in terms of country of origin, gender, stunting status, and age as well as potential biomarkers for EED are given in *SI Appendix*, Tables S1–S3. In 96 of 109 duodenal samples, we observed small intestinal overgrowth, of which 64 samples were from Bangui and 32 samples were from Madagascar. This suggests that the vast majority of stunted children (88.1%) suffer from SIBO. For 50 children (23 from Bangui and 27 from Antananarivo), we obtained valid sequencing data from all three sites along the gastrointestinal tract (gastric, duodenal,

and fecal samples), allowing us to further probe the underlying composition and causes of SIBO.

Gastrointestinal Sampling Site, Country of Origin, and Different Clinical Cofactors Modulate the Intestinal Microbiota. We first aimed to investigate the overall variation in the microbiota composition between the different study and sampling sites as well as in children with differing clinical cofactors. Sample composition varied between the two countries (Fig. 1 *A* and *C*) and among the different segments along the gastrointestinal tract (Fig. 1*B*, Datasets S4–S7, and *SI Appendix*, Fig. S1*A*), with *Fusobacteriales, Neisseriales, Pasteurellales,* and *Lactobacillales* vs. *Clostridiales* and *Bacteroidales*, among others, mainly driving the separation of samples from the upper and lower gastrointestinal tracts and a larger array of different orders driving the separation of the fecal samples between the two countries (*SI Appendix*, Fig. S2). Of note, *Bifidobacteriales* were more prevalent in fecal samples from Madagascar, where breastfeeding length is significantly longer than in the CAR. We further confirm our previous result (7) obtained on a subset of the samples regarding the over-representation of bacteria of oral origin in the duodenum and the
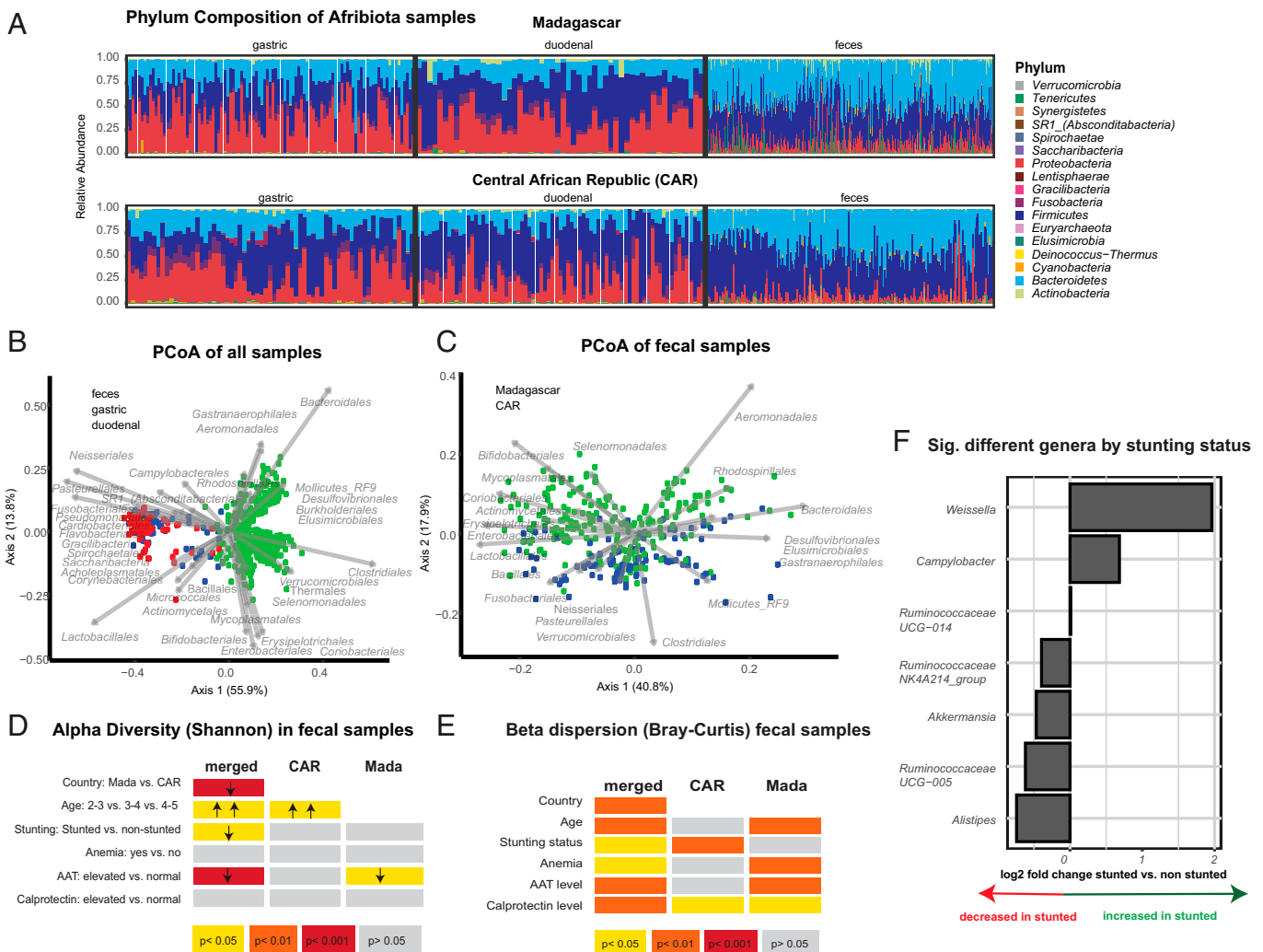
Fig. 1. Differences in the fecal microbiota induced by different clinical cofactors. (*A*) Relative phylum abundance of the different samples analyzed in this study. (*B*) PCoA (Principal Coordinate Analysis) on the Bray–Curtis dissimilarity index of the samples rarefied to 5,000 sequences. Gastric samples: $n = 212$; duodenal samples: $n = 137$; fecal samples: $n = 634$. (*C*) PCoA on the Bray–Curtis dissimilarity index of the fecal samples rarefied to 5,000 sequences. Bangui, Central African Republic: $n = 254$; Antananarivo, Madagascar: $n = 380$. Alpha-diversity (*D*) and beta-diversity (*E*) in the fecal microbiota and the independent association with given clinical cofactors. (*F*) Significantly different genera according to stunting status in a multivariate DeSeq2 analysis using a generalized linear model and a likelihood ratio test correcting for age, gender, country of origin, and sequencing run on the pooled dataset from Bangui and Antananarivo.

underrepresentation of putative butyrate-producing bacteria in feces of stunted children, compared with nonstunted controls (Fig. 1*F* and *SI Appendix*, Fig. S1*B*). In feces, we also observed a clear increase of the genus *Campylobacter* in the context of stunting in the CAR (*SI Appendix*, Fig. S1*B*). Alpha-diversity of the fecal samples, measured through the Shannon Diversity index, was mainly affected by country of origin and—driven by the samples from Madagascar—by age and alpha-antitrypsin (AAT) levels (Fig. 1*D*). Beta-dispersion was mainly driven by country of origin, fecal calprotectin levels, and the age of the children (Fig. 1*E*). Further, we observed a small but significant contribution of anemia to the beta-dispersion of the fecal samples in the merged dataset as well as in the dataset from Madagascar, while stunting status was only a significant driver in the CAR.

In conclusion, our data confirm our earlier results on the uniqueness of the small intestinal microbiota as well as the higher levels of oral bacteria and lower levels of butyrate producers in the feces of stunted children compared with nonstunted controls and show a clear effect of country of origin on the microbial profile. Further, we demonstrate a negative association between intestinal inflammation, anemia, and overall fecal microbiota diversity.

Candidate Biomarkers of EED Are Associated with a Distinct Fecal Bacterial Signature in the Feces. EED is suspected to be a main driver of stunting in developing countries. While there is

to date no validated biomarker for the disease, intestinal inflammation is widely accepted as the most robust readout (14). To assess for microbial members associated with EED, we compared the fecal microbiota in children with normal or elevated levels of either fecal calprotectin, a marker of intestinal inflammation, or AAT, a marker of intestinal inflammation and protein-losing enteropathy. While the two markers were clearly positively correlated ($P < 0.001$ in a Spearman correlation test, rho = 0.41), a significant number of children showed only elevated levels of AAT (8.4%) or calprotectin (16.95%) vs. children with both markers concomitantly elevated (7.7%) or both markers in the normal range (66.95%). We thus analyzed the effect of both markers separately from each other. Of note, none of the two markers were associated with stunted child growth.

We next investigated if there was an association between overall fecal microbiota composition and fecal AAT/calprotectin levels. While only AAT was associated with a modest reduction in alpha-diversity in Madagascar (Figs. 1*D* and 2*A*), AAT and especially, calprotectin levels appeared significantly and independently associated with beta-dispersion (Fig. 1*E*). *Fusobacterium*, *Megasphaera*, and *Parabacteroides* were enriched in fecal samples of children with either elevated calprotectin levels and/or elevated AAT levels (Fig. 2 *B* and *C*). Further, in the children with elevated AAT levels, we observed significantly higher relative abundance of *Bifidobacterium* and *Collinsella* (Fig. 2*C*). In the context of elevated AAT and calprotectin
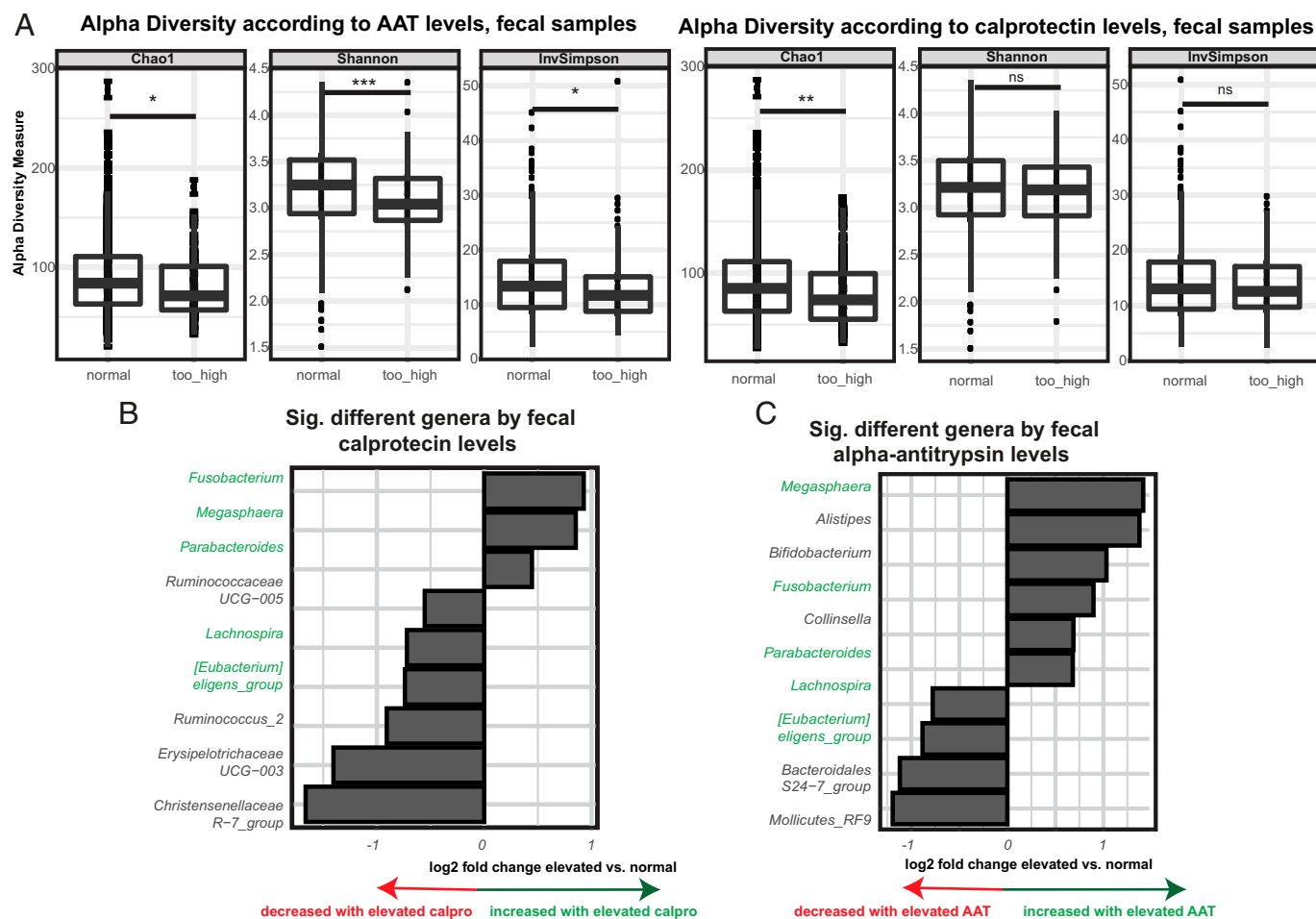
Fig. 2. Fecal inflammatory biomarkers of EED and their association with the fecal microbiota. (*A*) Alpha-diversity measures in fecal samples according to AAT and calprotectin levels. Significantly different genera according to (*B*) calprotectin levels and (*C*) AAT levels in a multivariate DeSeq2 analysis using a generalized linear model and a likelihood ratio test correcting for age, gender, country of origin, stunting status, and sequencing run on the pooled dataset from Bangui and Antananarivo. Taxa similarly affected by calprotectin and AAT are indicated in green. ns, $P > 0.05$. *$P < 0.05$; **$P < 0.01$; ***$P < 0.001$

levels and independently of stunting status, we observed in both countries a reduction in the relative abundance of *Clostridiales*. We also observed an increase in several genera, such as *Megasphaera* and *Fusobacterium*. While there were trends in the fecal samples from the CAR, these effects were mostly driven by the Malagasy samples (*SI Appendix*, Fig. S3). Overall characteristics of the study population and factors affecting the fecal microbiota are summarized in Fig. 1 and *SI Appendix*, Figs. S1–S3 and Tables S1–S3.

Thus, a specific fecal bacterial signature appears associated with fecal EED markers that is independent of the geographic origin or the stunting status of the children.

Duodenal Aspirates in Both Countries Display a Conserved Set of Bacterial Taxa and Show Distinct Clusters of Co-Occurring and Co-Excluding Strains. As nutrient absorption takes place in the small intestine, we assessed the small intestinal microbiota composition in the duodenum. For ethical reasons, we were only able to take duodenal samples from stunted children and to compare the community composition between severely and moderately stunted children. There was a clear shared core microbiota present in at least 90% of all duodenal samples at a relative abundance of >0.01% and a slightly extended microbiota present in at least 75% of all samples at a relative abundance of >0.01%. This core microbiota was largely the same in both study countries, with the *Deinococcus–Thermus* group being slightly more abundant in Madagascar (Fig. 3 *B* and *C*) ($P = 0.005$).

Co-occurrence analysis revealed clear groups of co-occurring and co-excluding taxa. At the lower taxonomic level, we observed two groups of co-occurring bacteria that are collectively co-exclusive (Fig. 3*D* and *SI Appendix*, Figs. S4 and S5)—typical oral bacteria, such as *Streptococcus*, *Staphylococcus*, *Moraxella*, *Canocytophaga*, or *Rothia*, and intestinal bacteria, such as *Prevotella*, *Alloprevotella*, *Ruminococcaceae*, or different *Lachnospiraceae*. This pattern was observed in both study countries independently (*SI Appendix*, Figs. S4 and S5). At a higher taxonomic level, we observed co-occurrence of *Actinobacteria*, *Clostridia*, and *Erysipelotrichia* in the duodenal samples, which was mutually exclusive with high levels of *Gammaproteobacteria* (Fig. 3*E*), especially in the CAR.

Country of origin was the only cofactor slightly influencing beta-dispersion of duodenal samples (explaining 2% of the total variability). Samples from Madagascar had slightly higher levels of *Proteobacteria* (especially *Neisseriales* and *Pasteurellales*) and slightly lower levels of the *Deinocuccus–Thermus* group and *Firmicutes* (Fig. 3*B* and *SI Appendix*, Fig. S2*C*).

Thus, we can define a conserved microbial signature in the small intestine of stunted children that is governed by patterns of co-occurrence and co-exclusion.

Characterization of the Gastric and Small Intestinal Microbiota in the Context of Stunting Severity and SIBO. We next aimed to assess changes in the community structure of the small intestinal microbiota in the context of moderate and severe stunting as well as SIBO, a hallmark of EED and stunting.

The duodenal samples were equally distributed between moderately and severely stunted children (*SI Appendix*, Table S2). Although we did not observe any differences in the small intestinal microbiota by stunting severity, SIBO had a significant impact on the duodenal and gastric microbiota (*SI Appendix*, Fig. S6).

SIBO was present in 66% of all stunted children from Madagascar who had a test performed and 84% of all children in the CAR (*SI Appendix*, Table S2). On average, we counted 2.1×10^6 colony-forming units (CFU)/mL in the samples from the CAR

(minimum: 0, maximum: 2.2×10^8, interquartile range [IQR]: 1.3×10^7) and 2.3×10^6 CFU/mL in the samples from Madagascar (minimum: 0, maximum: 1.6×10^8, IQR: 2.8×10^7). Assessing for differences in given species in the gastric samples, there was a clear decrease of several strict anaerobes in gastric samples from children suffering from SIBO (*SI Appendix*, Fig. S6 *B* and *C*) and an increase in *Helicobacter* and *Campylobacter* (driven by samples from Madagascar) (*SI Appendix*, Fig. S6 *A* and *B*). In the CAR, *Dolosigranulum pigrum* was significantly increased in duodenal aspirates of children with SIBO compared with children without SIBO, and *Helicobacter* was reduced (*SI Appendix*, Fig. S6*H*). In Madagascar, SIBO was associated with slightly higher levels of *Treponema* and lower levels of *Serratia* (*SI Appendix*, Fig. S6*I*). No conserved signatures were visible for changes in the relative abundance of given taxa at the genus level in the feces of children with SIBO compared with children without SIBO (*SI Appendix*, Fig. S6 *D–F*).

It has been previously shown that ectopic colonization with oral bacteria is associated with markers of EED in a mouse model (8). We thus aimed to assess if SIBO was associated with an increase in the small intestinal inflammatory state. To this purpose, we measured cytokine, AAT, and calprotectin levels in the small intestine (*SI Appendix*, Table S2). There was a statistically significant positive association between the duodenal levels of AAT, calprotectin, and cytokines in the CAR but not in Madagascar (*SI Appendix*, Fig. S7). Further, there was no association between fecal calprotectin/AAT and duodenal cytokines in any of the countries. While there were no changes in cytokines, AAT, or calprotectin in the duodenum by stunting severity (moderate vs. severe), there was a significant increase in several proinflammatory cytokines when children exhibited SIBO (Fig. 3*A*). This indicates that SIBO in stunted children is associated with increased small intestinal inflammation.

In conclusion, our data show that SIBO is associated with specific bacterial species in the upper gastrointestinal tract, with a small trend to the increased presence of potential proinflammatory strains and a small reduction in strict anaerobes. This inflammation does not seem to be strongly associated with the relative abundance of a specific bacterial taxon present but rather, a reflection of the overall community composition.

Ectopic Colonization with Small Intestinal Isolates of Oral Bacteria Leads to Diminished Lipid Absorption in Cultured Intestinal Cells. Using a small intestinal clinical isolate of *Streptococcus salivarius* as a model oral bacterium (strain AF5, *S. salivarius* II) (*SI Appendix*, Table S5), we assessed for a direct role in intestinal inflammation using either polarized murine intestinal m-IcCl2 cells or antibiotic pretreated mice (*Animal Experiments*). The *S. salivarius* strain tested was not associated with any change in inflammation (Figs. 4*B* and 5*D*).

We next assessed for a potential influence of small intestinal bacterial isolates on lipid absorption (Fig. 4*A* and *SI Appendix*, Fig. S8). To this purpose, we tested lipid uptake in murine small intestinal cells (m-IcCl2) exposed to a subset of clinical small intestinal isolates representing the main small intestinal taxa recovered (*SI Appendix*, Table S5) (15). All oral bacterial strains tested with the exception of *Lactobacillus paracasei*, a reference strain that showed no change in lipid absorption in previous work (12), significantly decreased ^{14}C–oleic acid absorption in m-IcCl2 cells compared with control conditions (Fig. 4*C*). This decrease was of higher magnitude in *S. salivarius* strains, particularly in *S. salivarius* II/strain AF5, and was independent of the growth velocity of the bacteria in the cell culture supernatant (*SI Appendix*, Fig. S8*B*). We then assessed if
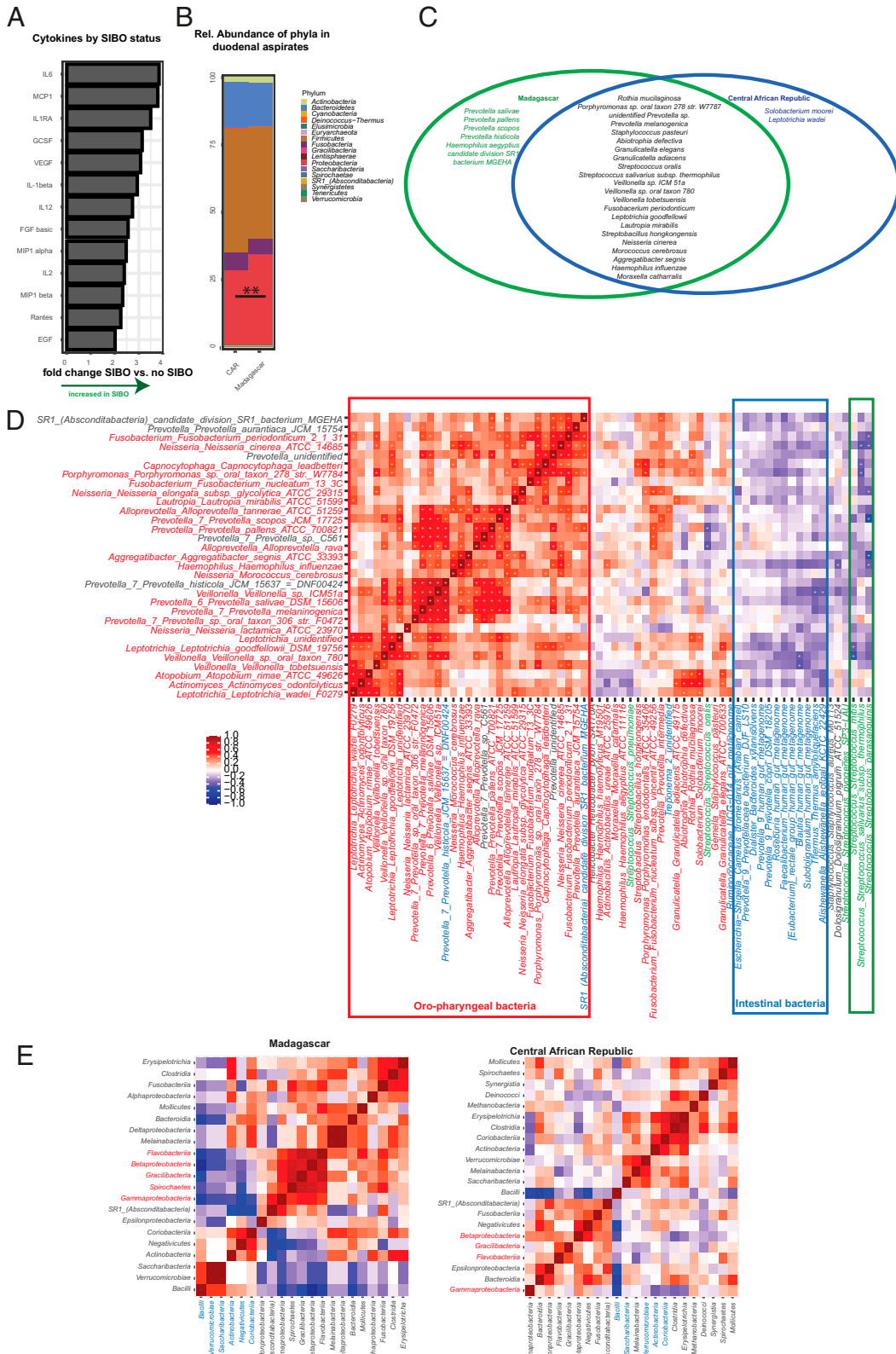
Fig. 3. Small intestinal microbiota in children suffering from stunted growth. (*A*) Cytokines with a significantly different relative abundance between duodenal samples from children suffering from SIBO compared with children not suffering from SIBO in a logistic regression correcting for analysis batch, country of origin, and the presence or absence of anemia and using the Benjamini–Hochberg correction. (*B*) Average phylum relative abundance in Bangui, CAR and Antananarivo, Madagascar. (*C*) Core species at 0.01% relative abundance and a minimal prevalence of 75% in Antananarivo, Madagascar (green) or Bangui, Central African Republic (blue) or conserved in between both study countries (black). (*D*) Heat map of the Spearman correlation of duodenal samples co-occurrence/co-exclusion including all species with a relative abundance of at least 0.1%. Co-occurrence is indicated in red, and co-exclusion is in blue. Significant associations are indicated with a plus sign. (*E*) Heat map of co-occurrence and co-exclusion of different classes in the small intestine as measured by Spearman correlation on the relative abundance of given bacterial classes. Only classes with at least 0.1% relative abundance were kept in the analysis. A plus indicates a significant interaction ($P < 0.05$). Positive associations are indicated in red, and negative associations are in blue. Co-occurrences in Malagasy samples are indicated in the *Left pannel* and co-occurrences in Central African samples are indicated in the *Right pannel*. ns, $P > 0.05$. *$P < 0.05$; **$P < 0.01$; ***$P < 0.001$

the bacteria affected enterocyte monolayer integrity by performing a sulfonic acid apical to basal permeability assay (Fig. 4D). Several of the clinical *Streptococcus* isolates led to a small yet significant increase in permeability (of 10%), suggesting that these bacteria could be directly contributing to the leaky gut syndrome. To identify the bacterial effectors by which *S. salivarius* II could alter enterocyte lipid metabolism, we tested the effect of live and heat-inactivated *S. salivarius* II, *S. salivarius* II culture supernatants, and pH 5 (media pH equivalent to that of *S. salivarius* II

culture supernatant [*SI Appendix*, Fig. S8B]) on lipid absorption and secretion in m-ICcl2 cells (Fig. 4E). Live *S. salivarius* II, *S. salivarius* II supernatant, and the fraction of supernatant containing molecules with a size smaller than 3 kDa decreased lipid absorption to a similar extent, while pH and heat-inactivated bacteria did not interfere with lipid absorption. As previously shown for *Escherichia coli* and *Lactobacillus paracasei* (11, 12), *S. salivarius* II and its metabolites further led to decreased lipid secretion in m-ICcl2 cells (Fig. 4F). We
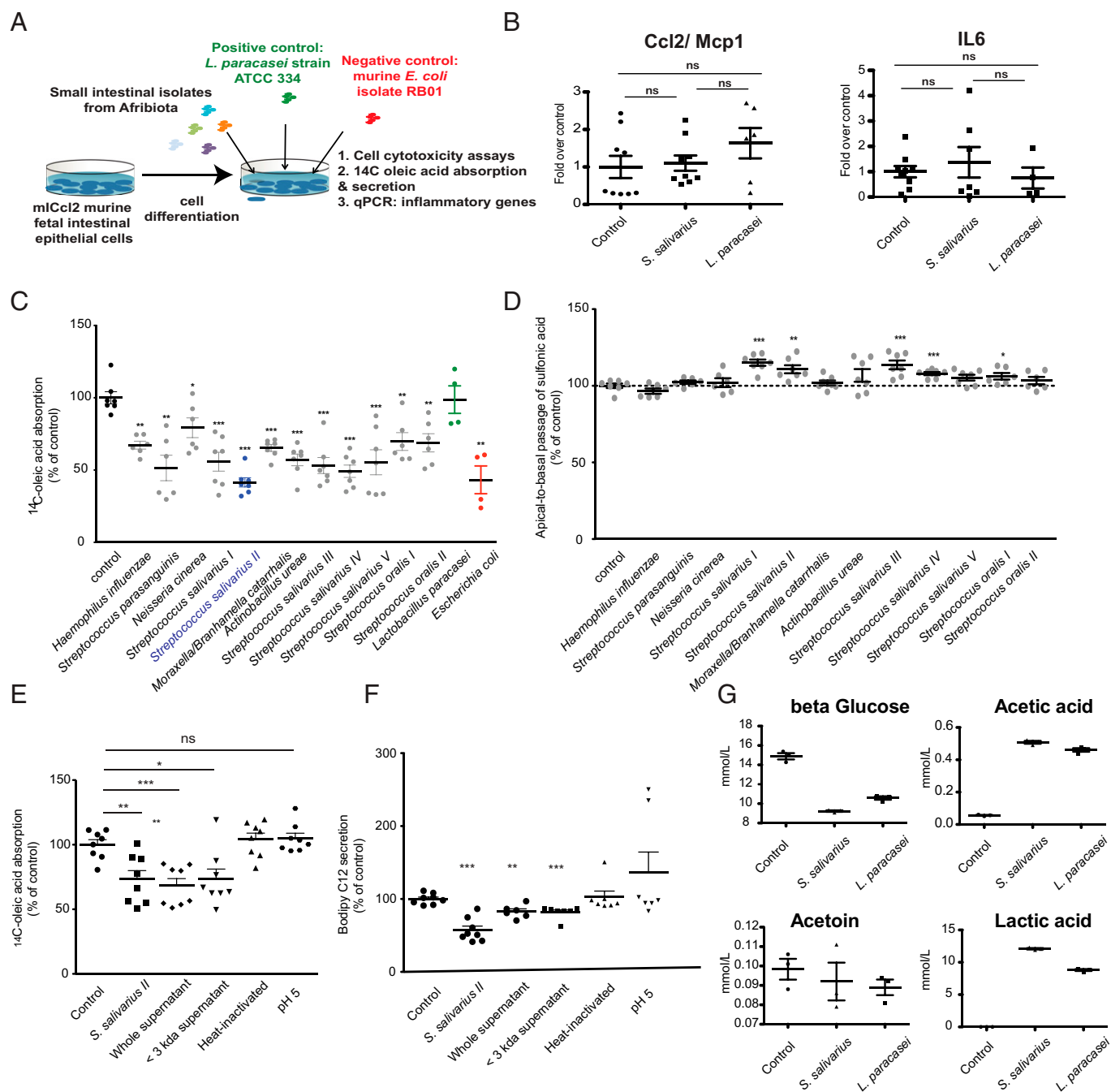
Fig. 4. Duodenal isolates of oropharyngeal bacteria lead to decreased lipid absorption in vitro. (A) Experimental setup of the in vitro cell assay. (B) Expression of proinflammatory genes in m-ICcl2 cells overexposed to either a clinical, small intestinal isolate of *S. salivarius* or *L. paracasei* (control bacterium). Values are normalized to the geometric mean of the three housekeeping genes *tbp*, *b2m*, and *gapdh*. (C) Oleic acid absorption in polarized murine small intestinal cells (m-ICcl2) cocultured overnight with different clinical isolates from the duodenum of stunted children. (D) The sulfonic acid apical to basal permeability assay in polarized m-ICcl2 cells cocultured overnight with different clinical isolates from the duodenum of stunted children. (E) Oleic acid absorption in the context of live *S. salivarius* strain II, whole or filtered culture supernatant, or heat-killed cells of *S. salivarius* II or in a medium acidified to pH 5. (F) BODIPY C$_{12}$ (lauric acid) secretion in the context of live *S. salivarius* strain II, whole or filtered culture supernatant, or heat-killed cells of *S. salivarius* II or in a medium acidified to pH 5. (G) NMR-quantified levels of metabolites in the supernatant of polarized m-ICcl2 cells cocultured for 16 h with control medium, *S. salivarius*, or *L. paracasei*. Experiments were performed in three independent replicates. Groups are compared using the Mann–Whitney *U* test. ns, $P > 0.05$. *$P < 0.05$; **$P < 0.01$; ***$P < 0.001$.

hypothesize that low–molecular weight fermentation end products secreted by *S. salivarius* II mediate their effects on enterocyte lipid metabolism. We next performed targeted NMR analysis of the main fermentation end products present in bacterial supernatants. There was no difference in the levels of any of the fermentation products we tested between supernatants of *S. salivarius* and *L. paracasei* (Fig. 4*G*), suggesting that yet another metabolite or small bacterial molecule is mediating this effect or—in the in vivo setting—that the effect is of quantitative nature rather than of qualitative nature as many of the children displayed up to 1,000× more bacteria in their small intestine compared with reference values.

Together, these in vitro results show that small intestinal isolates of oral bacteria, dominated by *S. salivarius*, decrease the absorption of lipids in intestinal epithelial cells.

Ectopic Colonization with *S. salivarius* II Leads to Diminished Lipid Absorption in the Small Intestine and Liver of Mice. We next aimed to validate these results in a mouse model (Fig. 5*A*). Mice were cleared of their microbiota using an antibiotic mixture containing vancomycin, neomycin, metronidazole, and amphotericin B (Fig. 5*B*) and gavaged over 3 d with the clinical isolate *S. salivarius* II (AF5; which showed the largest decrease in lipid absorption in the cell culture assay), *L. paracasei*, or phosphate buffer saline (PBS). Mice were quasimonocolonized with the respective strain and were quasimonocolonized by *Paenibacillus* sp. in the control group (Fig. 5 *C* and *E*). Mice treated with *S. salivarius* II displayed significantly lower levels of jejunal and liver BODIPY C_{12}-labeled fatty acids (Fig. 5*F*) and showed no signs of inflammation (Fig. 5*D*).

Together, these results show that *S. salivarius* II decreases intestinal absorption and consequently, liver accumulation of dietary fatty acids.

Discussion

Our results clearly show that stunted growth and/or EED are associated with specific changes in the bacterial community of the feces and that there are small intestinal bacterial changes associated with SIBO, which is pervasive in stunted children in this population. These bacterial changes are associated with low-level inflammation and—in experimental models—with gut leakiness and lipid malabsorption. We further confirm and expand our previous results, and we show that overgrowth by oral bacteria in the small intestine leads to a displacement of the classical small intestinal bacteria and that these clinical isolates are associated with low-grade inflammation and decreased lipid absorption in a cell culture model as well as in an animal model. The decrease in lipid absorption in small intestinal enterocytes is induced by the massive overgrowth by several phylogenetically different oral bacteria. These small intestinal bacteria from stunted patients were associated with changes in nutrient absorption; this work, therefore, has important implications for a better understanding of microbiota–host interactions in the context of undernutrition and other diseases associated with ectopic colonization of oral bacteria.

Chronic low-grade inflammation and overproduction of metabolic products reducing lipid absorption may complement each other as their respective intensity may vary among stunted children.

Our clinical results show that a low-grade intestinal inflammation occurs in the duodenum of children with SIBO, involving elevated levels of duodenal AAT and calprotectin as well as several cytokines, including IL-6 and Mcp1. We were unable to link a single bacterial taxon to the phenomenon, suggesting that a group of bacteria rather than a single taxon is driving the proinflammatory state. This is in line with work in Bangladesh,
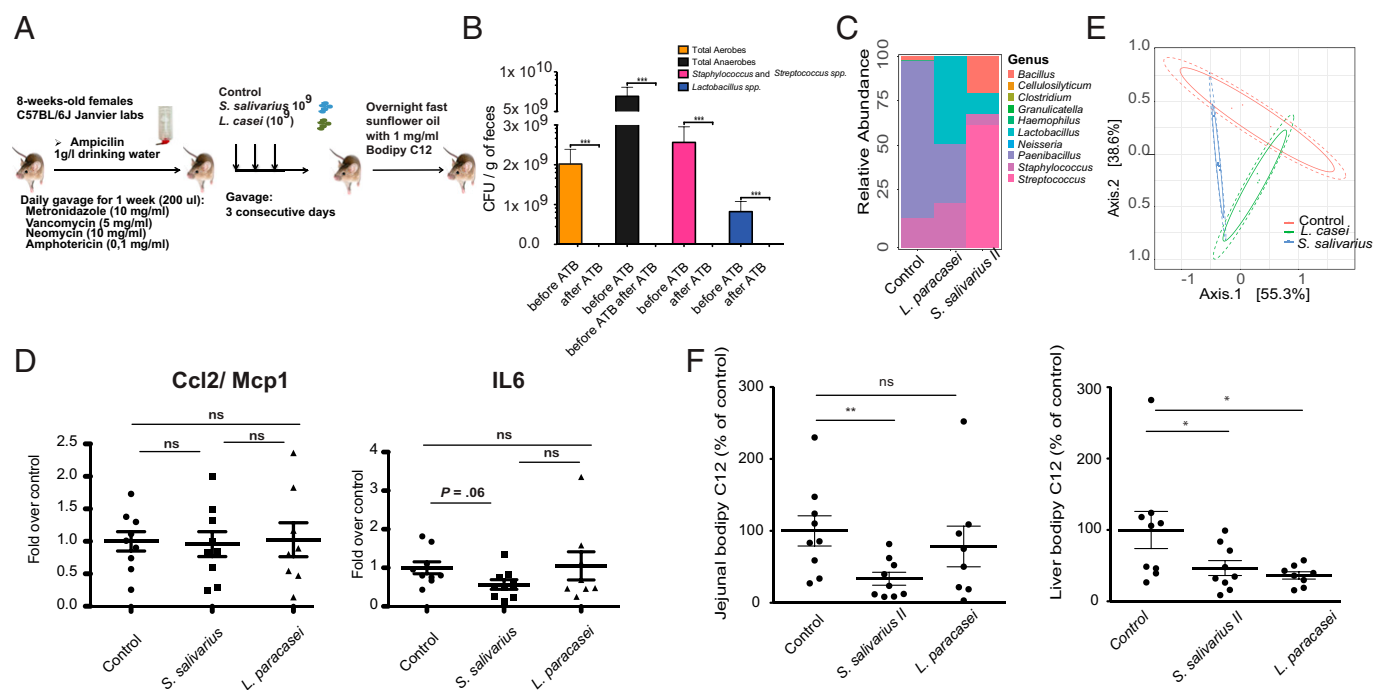
Fig. 5. Duodenal isolates of oropharyngeal bacteria lead to decreased lipid absorption in vivo. (*A*) Schema of the experimental setup of the mouse experiments performed. (*B*) CFU for different groups of bacteria in the feces of mice prior to and after treatment with the antibiotic mixture for 7 consecutive days. (*C*) Average relative abundance of bacterial genera in the three treatment groups. (*D*) Expression of proinflammatory genes in the small intestine of mice overexposed to either *S. salivarius* or *L. paracasei* (control bacterium). Values are normalized to the geometric mean of the three housekeeping genes *tbp*, *b2m*, and *gapdh*. (*E*) PCoA (Principal Coordinate Analysis) on the Bray–Curtis index of the 16S amplicon data of the three treatment groups on ASV level; 95% CIs of the beta-dispersion of a given sample group are indicated with two ellipses. (*F*) BODIPY C_{12} absorption in the jejunum and liver of mice overexposed to *S. salivarius* or *L. paracasei*. Groups are compared using the Mann–Whitney *U* test. ATB, antibiotics. ns, $P > 0.05$. *$P < 0.05$; **$P < 0.01$; ***$P < 0.001$.

showing a role for the absolute abundance of a consortium of 14 oral bacteria in small intestinal inflammation in a mouse model of undernutrition (8).

Further, the microbiota analysis in the small intestine reveals that there are opposite relative abundances between putative oral species (defined in the Human Oral Microbiome Database) as well as classical fecal bacteria. Displacement of the typical intestinal microbiota with bacteria normally found in the oral cavity has also been described in inflammatory bowel disease; ectopic colonization by oral bacteria is further associated with colorectal cancer as well as liver disease (reviewed in ref. 16), but it remains debated if this disbalance is due to inflammation induced by the oral bacteria or through driving of the oral bacteria in the context of inflammation. Previous work suggests a link between *Helicobacter pylori* infection and gastric pH (17). We did not see any significant association between SIBO and gastric pH nor SIBO and *Helicobacter* infection and only a small trend to lower pH with higher relative abundance of *Helicobacter*. Nevertheless, as we did not specifically targeted *Helicobacter* using, for example, qPCR to assess for absolute bacterial load and only assessed pH using pH paper, these results might not be robust and should be verified in a dedicated study.

In addition to changes in the small intestine, we could show that markers of EED are also associated with changes in the fecal microbiota. In our study, EED markers were associated with elevated fecal levels of *Fusobacterium*, *Megasphaera*, and *Collinsella* and lower levels of strict anaerobic butyrate producers. An earlier study that assessed EED-associated bacteria in feces in Malawi and focused on lactulose–mannitol absorbance as a proxy for gut leakiness and EED (18) found that *Megasphaera*, *Mitsuokella*, and *Sutterella* were more abundant in the feces of children with EED, whereas *Klebsiella* and *Clostridium_XI* were less abundant; this is consistent with our observation of more inflammation-associated taxa and less butyrate-producing *Clostridia* in the feces of children with EED. Considering that in our study population, virtually all children displayed elevated gut leakiness, we were unable to repeat the analysis with the same biomarker that the previous studies used. Interestingly, three of the taxa elevated in children with EED (*Fusobacterium*, *Megasphaera*, and *Collinsella*) are known to also be overrepresented in feces of patients suffering from other inflammatory disease, such as colorectal cancer (19, 20), active Crohn's disease (21), celiac disease (22), and/or nonalcoholic steatohepatosis (23). It remains unclear, however, whether these bacteria are causally implicated in disease or if they merely thrive better in the context of gut inflammation (24, 25). Several taxa, including *Bilophila wadworthia* (26) and *Collinsella* (27), have also been implicated in metabolic disease, suggesting a role for these bacteria in the double burden of undernutrition and EED in early life and metabolic disease in later life. Further, our study highlights the overrepresentation of *Campylobacter* in stunted children independently of the country, adding to the growing literature associating asymptomatic *Campylobacter* carriage with stunted child growth (7, 28–31).

In addition, our work has unraveled a second unrelated driver of malnutrition in stunting: the reduction of lipid absorption by bacteria isolated from the small intestine of stunted children, which we have shown both in a cell culture as well as in an animal model. Due to the lack of small intestinal biopsies from these children, we were, however, unable to assess this phenomenon directly in the affected children. Future studies should also assess for blood lipid profiles and spot fecal fat or calorimetry in fecal samples to assess for lipid status directly in the affected children and strengthen the link between small intestinal microbial shifts, lipid malabsorption, and EED.

Recent data in duodenal biopsies from EED children from Pakistan (32, 33) show changes in lipid absorption and metabolism pathways as well as changes in duodenal and serum bile acid profiles and signals for dysbiosis (i.e., up-regulation of DUOX2) and fecal energy loss. Most interestingly, fecal energy loss and inflammation partially improved in children in a randomized control trial testing alanyl-glutamine as a gut repair nutrient for an intervention of 10 days (34). Previous work also found an association between *Giardia* infestation and steatorrhea (35, 36), a parasite that is frequently found in low- and middle-income countries (37–39). However, no association with stunting was found in the population of children studied here (38).

A direct role for commensal bacteria in lipid metabolism has previously been described by our group for *E. coli* (11, 12) and *L. paracasei* (11, 12) and also suggested for *Clostridiales* (40, 41) and *Desulfovibrio* (40). Previous work by our group has shown that the two commensals *L. paracasei* and *E. coli* alter lipid metabolism through the fermentation products L-lactate and acetate, respectively (12). More work is needed to elucidate the implicated metabolite and the cellular pathway by which the small intestinal clinical isolates lead to decreased lipid absorption and to assess the role of these bacteria directly in affected children.

Lipid absorption and inflammation most likely independently contribute to the pathophysiology underlying stunted child growth. They are also indirectly linked as inflammation modulates the composition of the microbiome, which in turn, then interacts with lipid absorption and storage (11, 12, 41). In our experimental study, in contrast to our clinical data to a previous study in Bangladesh (8), the oral clinical isolate tested was not able to induce inflammation, suggesting that different members of the SIBO community contribute to different aspects of the EED pathophysiology. Our results on inflammation are limited by the fact that only a single strain was tested for proinflammatory potential. More research on small intestinal bacterial isolates is needed to better understand what is driving inflammation in the small intestine of stunted children. Malabsorption could hence be inversely influenced through low-level inflammation induced by specific bacterial taxa or communities and the presence of absorption-modulating bacteria, such as members of the oral microbiome.

Our study also has a few limitations, especially the fact that we were not able to assess for lipid absorption and lipid absorption–associated genes directly in epithelial tissues. Further, dosing short-chain fatty acids and providing absolute values on taxa abundance would give a better idea of the actual reduction in butyrate and the actual bacterial load. Further, steatorrhea might also directly contribute to microbiota changes in the colon, a hypothesis that was not tested in this study. These points should be addressed in future studies.

In conclusion, our study suggests an implication of ectopic colonization of oral bacteria in gut leakiness and nutrient malabsorption in vitro and confirms the association between SIBO and low-grade inflammation in stunted children. Further, we show a specific independent signature associated with EED markers in the large intestine, which is conserved in both study settings.

Tooth decay and oral health are of major concern in Africa and have been associated with malnutrition in Cambodia (42). In our study, more than a third of the participants in Madagascar showed visible caries (43), yet oral health was not associated with stunted growth. Our results show important avenues for the development of microbiota-targeted interventions. On the one hand, treating SIBO promises to decrease both small intestinal inflammation and lipid malabsorption. On the other hand, sustaining and replenishing members of *Clostridia* in the

large intestine promise to ameliorate colonization resistance and decrease inflammation in the large intestine. Clinical trials testing different microbiota-targeted interventions for the small and large intestine are clearly indicated (i.e., by ameliorating oral health and thus, preventing seeding of oral strains to the lower gastrointestinal tract and/or by boosting the growth of butyrate producers [i.e., through microbiota-directed foods and/or through specific prebiotics]). Such interventions are powerful candidates to ameliorate the treatment of stunting in the future.

Material and Methods

Study Setup, Collection of Samples and Metadata, and Biobanking. This transversal study was carried out in children living in four districts of Bangui, CAR or in two disadvantaged neighborhoods of Antananarivo, Madagascar. The study included children aged 2 to 5 years with no obvious signs of disease (bloody or mucus-containing diarrhea, signs of respiratory distress, HIV, wasting). All children recruited in the Afribiota project were eligible for this study. The detailed inclusion and exclusion criteria and recruitment procedures are described in ref. 13. Children were classified according to the median height of the WHO reference population (44) in three groups: severe stunting (height-for-age z score ≤ -3 SD), moderate stunting (height-for-age z score between -3 SD and -2 SD), and not stunted (height-for-age z score ≥ -2 SD) based on the cutoffs defined based on the WHO reference cohort (45). Metadata including nutritional status, iron levels, hemoglobin, age, and socioeconomic factors were collected with a standardized questionnaire. Complete blood count, C-reactive protein, and ferritin levels were measured at the Clinical Biology Center of the Institut Pasteur de Madagascar and the Laboratoire d'Analyze Médicale at the Institut Pasteur de Bangui within 4 h after blood collection according to accredited methods. Ferritin levels were corrected for systemic inflammation as described in ref. 46. Hemoglobin values of Malagasy children were adjusted for altitude as described in refs. 47 and 48, and anemia was defined as less than 110 g of Hb/L of blood according to the WHO criteria (45, 49).

Gastric, duodenal, and fecal sample collection was performed as described previously (7).

Caregivers were instructed to collect the feces in the morning before coming to the hospital. Gastric and duodenal samples were collected using a pediatric nasogastric tube (Vygon, France) and were only collected for stunted children (ethical constraint). Once the gastric, duodenal, or fecal samples were collected, they were aliquoted, frozen at $-20\,°C$, and transferred the same day to a $-80\,°C$ freezer (Bangui) or directly snap frozen in liquid nitrogen and then transferred to a $-80\,°C$ freezer (Antananarivo). SIBO was assessed by culture as described in ref. 15 and defined as $>2 \times 10^5$ CFU/mL of duodenal liquid. DNA extraction was performed on site in Antananarivo and Bangui (see below), and DNA was shipped on dry ice. Biobanking and sample distribution were performed by the Unité de Bactériologie Expérimentale, Institut Pasteur de Madagascar; the Laboratoire d'Analyze Médicale, Institut Pasteur de Bangui; and the Clinical Investigation and Access to BioResources Platform at the Institut Pasteur, Paris. The study protocol for Afribiota was approved by the Institutional Review Board of the Institut Pasteur (2016-06/IRB) and the National Ethical Review Boards of Madagascar (55/MSANP/CE, 19 May 2015) and the CAR (173/UB/FACSS/CSCVPER/16). All participants received oral and written information about the study. The legal representatives of the children provided written consent to participate in the study.

DNA Extraction and Sequencing. Samples were extracted by commercial kits (QiaAmp cador Pathogen Mini or cador Pathogen 96 QIAcube HT Kit; Qiagen) following the manufacturer's recommendations with an additional bead-beating step to increase mechanical disruption. Samples were stored at $-80\,°C$ until sequencing. Extracted DNA samples were shipped to a commercial provider, where library generation and sequencing were performed (Microbiome Insights). Extraction protocols were compared in between the two study sites using a Zymogen Mock Community. Library preparation was performed as recommended by Kozich et al. (50) using primers v4.SA501 to v4.SA508 and v4.SA701 to v4.SA712. The amplicon library was sequenced on a MiSeq using the MiSeq 500 Cycle V2 Reagent Kit (250×2). Data are available on the ENA server under accession number PRJEB48119.

Bioinformatic and Biostatistic Analysis of the Microbiota Composition. Demultiplexed reads were obtained from the sequencing facility and were processed using the Dada2 pipelines developed by the Holmes laboratory with slight modifications [https://benjjneb.github.io/dada2/ (51)], and taxonomy was assigned using the Silva Database (version 128). Minimum sequence lengths of 240 bp for the forward reads and 220 bp for the reverse reads were set, no N was allowed, and maximum EE was set to six/eight (forward/reverse). The original average input of the sequencing dataset was of 38,140 sequences/sample (minimum: 117 sequences, maximum: 185,013 sequences). We filtered out reads with a relative abundance of less than 0.1%. After filtering and removal of the chimeric sequences, this yielded on average 27,058 sequences per sample. Only samples with a final sequence count of at least 5,000 sequences were kept in the analysis. The stunted vs. nonstunted groups were compared using Pearson's χ^2 test or the Fisher exact test for qualitative variables and the Student's t test or the Mann–Whitney U test for quantitative variables. Statistical analyses and visualizations of the microbial data were conducted in R version 3.4.1 using Phyloseq (52), vegan (53), DeSeq2 (54), and ggplot2 (55) packages. Alpha-diversity was quantified using the observed number of taxa, a measure of richness (Chao1 index), a measure of evenness (Simpson's diversity index $= 1 -$ Simpson's index), and the combined Shannon index using rarefied data. Tests of differences of alpha-diversity between samples were performed using the nonparametric multivariate analysis of variance with the function "adonis" in the R package vegan (53). P values were Benjamini–Hochberg corrected. Multivariate analyses of differentially abundant taxa were performed on pooled samples from both countries as well as on data from each country independently. Multivariate models were corrected for gender and age (in months) as well as country of origin and stratified on sample type and then, on country of origin. Models on the fecal samples were further corrected for intestinal inflammation (AAT levels and calprotectin levels).

The metadata, ASV table, and taxonomy table can be found in Datasets S1–S3. The code can be found in GitHub under the following link: https://github.com/VonaeschLabUNIL/Afribiota.

Culture of Duodenal Aspirates and Identification of Colonies. Duodenal samples were processed as described previously (7). Briefly, RCM-diluted duodenal aspirations were diluted and streaked on plates according to the protocol described in Chandra et al. (56). Reisolated colonies were identified by MALDI-TOF mass spectrometry (Bruker Biotyper; Bruker Daltonics and Antananarivo). Cultures were considered positive for SIBO if the total bacterial count was $\geq 2 \times 10^5$ CFU/mL of duodenal fluid (56). Only duodenal samples with a pH value of at least five were retained in the analysis, as lower pH values suggested that the probe was localized rather than in the stomach (recoiling of the probe).

LUMINEX Analysis of Duodenal Cytokines. LUMINEX analysis was performed at the Centre d'Immunologie Humaine of the Institut Pasteur using the commercial Cytokine 30-Plex Human Panel from Invitrogen according to the manufacturer's instructions. In brief, 200 μL of duodenal aspirate was homogenized in 1 mL of PBS containing Protease Inhibitor Mixture (Roche Diagnostics GmbH), incubated for 30 min on ice, and centrifuged for 10 min at $10,000 \times g$ at $4\,°C$ in a tabletop centrifuge. Cytokines were measured on the undiluted supernatant using the DropArray method (Curiox Biosystems Pte Ltd.) on a Bioplex 200 machine (LUMINEX) according to the manufacturer's instructions. Values were measured in duplicates, and all samples with more than 20% difference in between the two measurements or values above the standard curve were repeated. Values that repeatedly produced discordant results were imputed by the mean of each cytokine. Values repeatedly under the standard curve were imputed with half the minimum, and values repeatedly over the standard curve were imputed with double the maximum for this cytokine. Differences in cytokine composition between children suffering of moderate or severe stunting as well as SIBO or specific bacterial taxa were analyzed using R, the Wilcoxon rank-sum test for categorical variables, and Spearman correlations for continuous variables. All comparisons were corrected for multiple testing using the Benjamini–Hochberg correction.

Assessment of Intestinal Inflammation and Permeability. Fecal and duodenal calprotectin concentrations were assayed in duplicate by a "sandwich"-type enzyme-linked immunosorbent assay, which uses a polyclonal antibody system (Calprest; Eurospital) according to the manufacturer's instructions (measurement range: 15 to 5,000 μg/g). Fecal and duodenal AAT was measured using an

immunonephelemetric method adapted on the BN ProSpeco system (Siemens). Briefly, stool samples were diluted 1:5 in 0.15 M NaCl and then, shaken vigorously by the mean of a vortex until complete homogenization. The homogenate was centrifuged at 10,000 × *g* for 15 min at 4 °C, and the supernatant was used for analysis (analysis at dilutions 1:5 and 1:500 to avoid any prozone phenomena; measurement range: 0.01 to 20 mg/g) (57). For AAT, values below 1.25 mg/g of fecal dry weight or below 0.15 mg/g of fecal wet weight were considered normal. For calprotectin, thresholds were adapted to age and were considered normal if the calprotectin levels were below 150 mg/g of fecal wet weight for children aged 2 to 3 y and 100 mg/g of fecal wet weights for children aged 3 y and older.

Enterocyte Cell Line (m-IcCl2). The m-IcCl2 murine fetal intestinal epithelial cell line derived from small intestinal villi was obtained from the laboratory of Alain Vandewalle, Faculté de Médecine Xavier Bichat, Paris, France (11), and it was used between passages 6 and 16. Cells were maintained in a humidified atmosphere of 5% CO_2 and 95% air and were grown in advanced DMEM/F12 medium (Gibco) supplemented with 2% fetal calf serum (Eurobio), 2 mM glutamax, 20 mM Hepes (Gibco), 50 nM dexamethasone, 10 nM human epidermal growth factor, and 1 nM triiodothyronine (Sigma-Aldrich). For subculturing, cells were removed enzymatically (0.05% Trypsin–EDTA; Gibco; 10 min, 37 °C) and seeded on 12-well transwell plates (1.12 cm^2, Ø 12 mm; 0.4-µm pore size inserts; Corning Costar) at a density of 3×10^5 cells/mL The medium was changed every 2 to 3 days until complete cell differentiation (14 days).

Coculture Assay of Bacterial Strains with m-IcCl2 Cells. *L. paracasei* WT strain ATCC 334 (formerly referred to as *Lactobacillus casei* ATCC 334) and the nonpathogenic murine *E. coli* RB01 isolate (11) were grown at 37 °C under aerobic atmosphere in MRS and LB medium, respectively (Difco). Bacterial strains isolated from duodenal samples of children were grown at 37 °C under aerobic atmosphere in the absence (*S. salivarius*) or the presence of 5% CO_2 (*SI Appendix*, Table S5 has details). Bacterial growth rates for the different strains were within a log except for *Moraxella catarrhalis*, for which we recovered roughly two log less bacteria in the cellular supernatant. Bacteria in stationary growth phase were harvested by centrifugation, washed with PBS, and resuspended in m-IcCl2 cell medium at a density of 3×10^5 CFU/mL except for strain AF2, which was resuspended at a density of 1.5×10^6 CFU/mL, and strains AF1 and AF3, which were resuspended at a density of 3×10^7 CFU/mL. Bacteria were then cocultured with m-IcCl2 cells in the apical compartment for 16 h. For the mouse experiments, *S. salivarius* II was grown to stationary growth phase, harvested by centrifugation, washed with PBS, and resuspended in PBS at a density of 10^9 CFU/mL.

m-IcCl2 Monolayer Integrity. The integrity of the m-IcCl2 cell monolayer was determined by two methods: the CytoTox 96 cytotoxicity assay according to the manufacturer's protocol (Promega) and measurement of the apical to basal permeability of sulfonic acid as described in ref. 12. Concerning the latter method, phenol red–free media containing sulfonic acid (200 µg/mL; Thermo Fisher Scientific) and bacteria were placed on the apical compartment, and phenol red–free media were placed on the basal compartment. After 16 h, the fluorescence of sulfonic acid (excitation at 485 nm and emission at 530 nm) on the basal compartment was measured with a TECAN Infinite M200 Pro plate reader (Tecan Austria GmbH).

^{14}C–Oleic Acid Absorption. After a 16-h treatment with bacteria or their supernatants, m-IcCl2 cells were washed three times with PBS and incubated on the apical compartment with 150 µL of serum-free culture medium containing 0.1% bovine serum albumin (BSA) free of fatty acids and 5 µM ^{14}C–oleic acid (Perkin-Elmer) for 2 min. The choice of this incubation time was based on previous time course experiments showing that ^{14}C–oleic acid absorption in m-IcCl2 cells was linear for up to 2 min (*SI Appendix*, Fig. S8A). After this period, absorption was stopped by removing the medium, washing cells three times with ice-cold PBS containing 0.1% BSA free of fatty acids, and placing them on ice. Cells were then solubilized with 225 µL of 0.1% (vol/vol) Triton X-100 (in 5 mmol/L Tris·HCl, pH 7.4) and left at 4 °C overnight. Intracellular radioactivity was measured by liquid scintillation counting and normalized for total cell protein determined by the EZQ Protein Quantitation Kit (Invitrogen) according to the manufacturer's protocol.

Lipid Secretion Assay. After a 16-h exposure of m-IcCl2 cells to bacteria or their supernatants, medium of the apical compartment was replaced by serum-free medium containing lipid micelles, which consisted of 0.6 mM oleic acid, 2 mM sodium taurocholate, 0.2 mM 2-mono-oleoylglycerol, 0.05 mM CHOL, 0.2 mM L-α-lysophosphatidylcholine (Sigma-Aldrich), and 0.02 mM BODIPY C_{12} fatty acid. Following a 10-min incubation, the medium containing micelles was removed and replaced by regular serum-free medium. Six hours after the addition of micelles, the fluorescence in the basal compartment was measured using a TECAN Infinite M200 Pro plate reader.

NMR Quantification of Fermentative Products. For analysis of bacterial metabolites, bacteria were incubated at 10^5 CFU/mL in advanced DMEM without glucose and any other additives. Quantifications were performed at the metabolomics platform of the University of Nantes (Capacités Spectrométrise) using NMR; 1D 1H spectra of cell culture supernatants from polarized m-IcCl2 cells were exposed during 16 h to control medium, *S. salivarius* strain II, or *L. paracasei*. Spectra were acquired on a Bruker 700-mHz spectrometer with a inversed 1H/13C 5-mm cryogenic probe. The following metabolites were quantified: lactic acid, acetic acid, acetoin, diacetyl, and glucose. Briefly, samples stored at −80 °C were thawed for 30 min at ambient temperature, 500 µL of supernatant was mixed with 35 µL of buffer solution (pH 2, reference for chemical displacement) and 30 µL of TSP solution (internal control, [TSP] = 28,83 mmol L^{-1}). After homogenization, pH was adjusted using hydrochloric acid to reach a final pH between 1.95 and 2.05. Samples were frozen again at −20 °C prior to NMR analysis. The day of the NMR measurement, the samples were thawed for 30 min at room temperature, homogenized, and introduced in an NMR cuvette. Spectra were acquired and treated with the Topsin 3.2 software using a recuperation delay of 35 s and a number of accumulations set to 128. The area under the curve for each metabolite was determined using the software AMIX.

Animal Experiments. Animal experiments were performed in compliance with French and European legislation on the care and protection of laboratory animals (EC Directive 2010/63, French Law 2013-118, 6 February 2013). All experiments were approved by the Ethics Committee of Institut Pasteur and by the French Ministry of Agriculture (reference no. 2015-0027). C57BL/6JR specific pathogen–free (SPF) mice (8-wk-old females) were purchased from Janvier Labs and were housed in the animal facility of Institut Pasteur. SPF mice were fed a regular chow diet and administered a microbiota-depleting antibiotic treatment for 8 d, consisting of a daily administration, by gavage, of a mixture of 5 mg/mL vancomycin (Acros Organics), 10 mg/mL neomycin, 10 mg/mL metronidazole (Sigma-Aldrich), and 0.1 mg/mL amphotericin B (Dominique Dutscher) resuspended in water. A gavage volume of 10 mL/kg body weight was administered with a stainless steel tube without prior sedation of the animals. One gram per liter ampicillin (Sigma-Aldrich) was also present in the drinking water. Fresh antibiotics were mixed every day, and ampicillin-containing water was renewed every 2 d. The day after the 8-d antibiotic treatment, fresh stools were collected for bacterial counts in order to confirm the efficacy of antibiotics, and mice were randomly assigned to three experimental groups ($n = 4$ to 5 per group). Mice were orally gavaged with 0.2 mL of PBS (control), *S. salivarius* II (10^9 CFU/d), or *L. paracasei* WT (10^9 CFU/d) during 3 consecutive days. After the 3-d treatment (12th day), overnight-fasted mice were orally gavaged with a bolus of 0.2 mL sunflower oil (Sigma-Aldrich) containing 1 mg/mL BODIPY 558/568 C_{12} (Thermo Fisher Scientific). After 1 h, mice were killed by cervical dislocation, and blood, jejunum, distal ileum (containing the luminal content), and liver (left lateral lobe) were immediately recovered for BODIPY C_{12} quantification, histological procedures, and/or CFU counts. BODIPY C_{12} fluorescence present in plasma and jejunal, distal ileum, and liver homogenates was measured using a TECAN Infinite M200 Pro (Tecan Austria GmbH; excitation at 548 nm and emission at 578 nm).

Data, Materials, and Software Availability. The 16S sequence data have been deposited in ENA (accession no. PRJEB27868) (58). All code has been deposited in GitHub under https://github.com/VonaeschLabUNIL/Afribiota (59). The bacterial strains isolated in this study are protected through a tripartite Charta by the Institut Pasteur, the Institut Pasteur de Madagascar, and the Institut Pasteur de Bangui, which foresees prior validation of the research by a scientific commission and establishment of an MTA. Any request for reagents should be addressed to the corresponding authors, who will then relate the information

to the scientific advisory board and inform interested parties about the steps to take. All other data are included in the article and/or supporting information.

Author affiliations: [a]Unité de Pathogénie Microbienne Moléculaire, Institut Pasteur, 75015 Paris, France; [b]Chaire de Microbiologie et Maladies Infectieuses, Collège de France, Paris, 75005 France; [c]Department of Epidemiology and Public Health, Swiss Tropical and Public Health Institute, Allschwil, 4123 Switzerland; [d]Department of Fundamental Microbiology, University of Lausanne, Lausanne, 1015 Switzerland; [e]University of Basel, Basel, 4001, Switzerland; [f]Complexe Hospitalo-Universitaire Pédiatrique de Bangui, Bangui, Central African Republic; [g]Laboratoire d'Analyse Médicale, Institut Pasteur de Bangui, Bangui, Central African Republic; [h]Unité de Bactériologie Expérimentale, Institut Pasteur de Madagascar, Antananarivo, 101 Madagascar; [i]Centre Hospitalier Universitaire Joseph Ravoahangy Andrianavalona; Antananarivo, 101 Madagascar; [j]Translational Immunology Laboratory, Institut Pasteur, 75015 Paris, France; [k]Unité d'Epidémiologie et de Recherche Clinique, Institut Pasteur de Madagascar, Antananarivo, 101 Madagascar; [l]Laboratoire de Coprologie Fonctionnelle, Assistance Publique-Hôpitaux de Paris, Hôpital Pitié-Salpêtrière, Paris, 75013 France; [m]Unité d'Epidémiologie, Institut Pasteur de Bangui, Bangui, Central African Republic; [n]Michael Smith Laboratory, Department of Microbiology and Immunology, University of British Columbia, Vancouver, BC, BC V6T 1Z4 Canada; and [o]Biodiversity Center, University of British Columbia, Vancouver, BC, BC V6T 1Z4 Canada

1. A. J. Prendergast, J. H. Humphrey, The stunting syndrome in developing countries. *Paediatr. Int. Child Health* **34**, 250–265 (2014).
2. J. C. Wells *et al.*, The double burden of malnutrition: Aetiological pathways and consequences for health. *Lancet* **395**, 75–88 (2020).
3. K. G. Dewey, S. Adu-Afarwuah, Systematic review of the efficacy and effectiveness of complementary feeding interventions in developing countries. *Maternal Child Nutr.* **4**, 24–85 (2008).
4. M. I. Smith *et al.*, Gut microbiomes of Malawian twin pairs discordant for kwashiorkor. *Science* **339**, 548–554 (2013).
5. S. Subramanian *et al.*, Persistent gut microbiota immaturity in malnourished Bangladeshi children. *Nature* **510**, 417–421 (2014).
6. L. V. Blanton *et al.*, Gut bacteria that prevent growth impairments transmitted by microbiota from malnourished children. *Science* **351**, aad3311 (2016).
7. P. Vonaesch *et al.*; Afribiota Investigators, Stunted childhood growth is associated with decompartmentalization of the gastrointestinal tract and overgrowth of oropharyngeal taxa. *Proc. Natl. Acad. Sci. U.S.A.* **115**, E8489–E8498 (2018).
8. R. Y. Chen *et al.*, Duodenal microbiota in stunted undernourished children with enteropathy. *N. Engl. J. Med.* **383**, 321–333 (2020).
9. J. Louis-Auguste, P. Kelly, Tropical enteropathies. *Curr. Gastroenterol. Rep.* **19**, 29 (2017).
10. R. J. Crane, K. D. Jones, J. A. Berkley, Environmental enteric dysfunction: An overview. *Food Nutr. Bull.* **36** (1 suppl.), S76–S87 (2015).
11. A. Tazi *et al.*, Disentangling host-microbiota regulation of lipid secretion by enterocytes: Insights from commensals *Lactobacillus paracasei* and *Escherichia coli*. *MBio* **9**, 59 (2018).
12. J. R. Araújo *et al.*, Fermentation products of commensal bacteria alter enterocyte lipid metabolism. *Cell Host Microbe* **27**, 358–375.e7 (2020).
13. P. Vonaesch *et al.*; AFRIBIOTA Investigators, Identifying the etiology and pathophysiology underlying stunting and environmental enteropathy: Study protocol of the AFRIBIOTA project. *BMC Pediatr.* **18**, 236 (2018).
14. K. M. Harper, M. Mutasa, A. J. Prendergast, J. Humphrey, A. R. Manges, Environmental enteric dysfunction pathways and child stunting: A systematic review. *PLoS Negl. Trop. Dis.* **12**, e0006205 (2018).
15. J. M. Collard *et al.*; Afribiota Investigators, High prevalence of small intestine bacteria overgrowth and asymptomatic carriage of enteric pathogens in stunted children in Antananarivo, Madagascar. *PLoS Negl. Trop. Dis.* **16**, e0009849 (2022).
16. E. Read, M. A. Curtis, J. F. Neves, The role of oral bacteria in inflammatory bowel disease. *Nat. Rev. Gastroenterol. Hepatol.* **18**, 731–742 (2021).
17. P. R. Harris *et al.*, *Helicobacter pylori*-associated hypochlorhydria in children, and development of iron deficiency. *J. Clin. Pathol.* **66**, 343–347 (2013).
18. M. I. Ordiz *et al.*, Environmental enteric dysfunction and the fecal microbiota in Malawian children. *Am. J. Trop. Med. Hyg.* **96**, 473–476 (2017).
19. M. H. Fukugaiti *et al.*, High occurrence of *Fusobacterium nucleatum* and *Clostridium difficile* in the intestinal microbiota of colorectal carcinoma patients. *Braz. J. Microbiol.* **46**, 1135–1140 (2015).
20. K. Mima *et al.*, Fusobacterium nucleatum in colorectal carcinoma tissue and patient prognosis. *Gut* **65**, 1973–1980 (2016).
21. A. Metwaly *et al.*, Integrated microbiota and metabolite profiles link Crohn's disease to sulfur metabolism. *Nat. Commun.* **11**, 4322 (2020).
22. R. Bodkhe *et al.*, Comparison of small gut and whole gut microbiota of first-degree relatives with adult celiac disease patients and controls. *Front. Microbiol.* **10**, 164 (2019).
23. S. Astbury *et al.*, Lower gut microbiome diversity and higher abundance of proinflammatory genus *Collinsella* are associated with biopsy-proven nonalcoholic steatohepatitis. *Gut Microbes* **11**, 569–580 (2020).
24. R. Sinha *et al.*, Fecal microbiota, fecal metabolome, and colorectal cancer interrelations. *PLoS One* **11**, e0152126 (2016).
25. E. L. Amitay *et al.*, Fusobacterium and colorectal cancer: Causal factor or passenger? Results from a large colorectal cancer screening study. *Carcinogenesis* **38**, 781–788 (2017).
26. J. M. Natividad *et al.*, Bilophila wadsworthia aggravates high fat diet induced metabolic dysfunctions in mice. *Nat. Commun.* **9**, 2802 (2018).
27. L. F. Gomez-Arango *et al.*, Low dietary fiber intake increases Collinsella abundance in the gut microbiota of overweight and obese pregnant women. *Gut Microbes* **9**, 189–201 (2018).
28. J. da Silva Quetz *et al.*, *Campylobacter jejuni* and *Campylobacter coli* in children from communities in Northeastern Brazil: Molecular detection and relation to nutritional status. *Diagn. Microbiol. Infect. Dis.* **67**, 220–227 (2010).
29. D. M. Dinh *et al.*, Longitudinal analysis of the intestinal microbiota in persistently stunted young children in South India. *PLoS One* **11**, e0155405 (2016).
30. Y. Terefe *et al.*, Co-occurrence of *Campylobacter* species in children from Eastern Ethiopia, and their association with environmental enteric dysfunction, diarrhea, and host microbiome. *Front. Public Health* **8**, 99 (2020).
31. G. Lee *et al.*, Effects of *Shigella*-, *Campylobacter*- and ETEC-associated diarrhea on childhood growth. *Pediatr. Infect. Dis. J.* **33**, 1004–1009 (2014).
32. Y. Haberman *et al.*, Mucosal genomics implicate lymphocyte activation and lipid metabolism in refractory environmental enteric dysfunction. *Gastroenterology* **160**, 2055–2071.e0 (2021).
33. X. Zhao *et al.*, Bile acid profiling reveals distinct signatures in undernourished children with environmental enteric dysfunction. *J. Nutr.* **151**, 3689–3700 (2021).
34. S. R. Moore *et al.*, Intervention and mechanisms of alanyl-glutamine for inflammation, nutrition, and enteropathy: A randomized controlled trial. *J. Pediatr. Gastroenterol. Nutr.* **71**, 393–400 (2020).
35. M. E. Ament, C. E. Rubin, Relation of giardiasis to abnormal intestinal structure and function in gastrointestinal immunodeficiency syndromes. *Gastroenterology* **62**, 216–226 (1972).
36. H. Troeger *et al.*, Effect of chronic Giardia lamblia infection on epithelial transport and barrier function in human duodenum. *Gut* **56**, 328–335 (2007).
37. K. L. Kotloff *et al.*, Burden and aetiology of diarrhoeal disease in infants and young children in developing countries (the Global Enteric Multicenter Study, GEMS): A prospective, case-control study. *Lancet* **382**, 209–222 (2013).
38. A. Habib *et al.*; Afribiota Investigators, High prevalence of intestinal parasite infestations among stunted and control children aged 2 to 5 years old in two neighborhoods of Antananarivo, Madagascar. *PLoS Negl. Trop. Dis.* **15**, e0009333 (2021).
39. S. Breurec *et al.*, Etiology and epidemiology of diarrhea in hospitalized children from low income country: A matched case-control study in Central African Republic. *PLoS Negl. Trop. Dis.* **10**, e0004283 (2016).
40. C. Petersen *et al.*, T cell-mediated regulation of the microbiota protects against obesity. *Science* **365**, eaat9351 (2019).
41. K. Martinez-Guryn *et al.*, Small intestine microbiota regulate host digestive and absorptive adaptive responses to dietary lipids. *Cell Host Microbe* **23**, 458–469.e5 (2018).
42. E. P. Renggli *et al.*, Stunting malnutrition associated with severe tooth decay in Cambodian toddlers. *Nutrients* **13**, 290 (2021).
43. P. Vonaesch *et al.*; AFRIBIOTA Investigators, Factors associated with stunted growth in children under five years in Antananarivo, Madagascar and Bangui, Central African Republic. *Matern. Child Health J.* **25**, 1626–1637 (2021).
44. World Health Organization, *WHO Child Growth Standards: Head Circumference-for-Age, Arm Circumference-for-Age, Triceps Skinfold-for-Age and Subscapular Skinfold-for-Age: Methods and Development* (World Health Organization, Geneva, Switzerland, 2007).

45. M. Onis; WHO Multicentre Growth Reference Study Group, WHO Child Growth Standards based on length/height, weight and age. *Acta Paediatr. Suppl.* **450**, 76–85 (2006).

46. D. I. Thurnham *et al.*, Adjusting plasma ferritin concentrations to remove the effects of subclinical inflammation in the assessment of iron deficiency: A meta-analysis. *Am. J. Clin. Nutr.* **92**, 546–555 (2010).

47. Centers for Disease Control (CDC), CDC criteria for anemia in children and childbearing-aged women. *MMWR Morb. Mortal. Wkly. Rep.* **38**, 400–404 (1989).

48. K. M. Sullivan, Z. Mei, L. Grummer-Strawn, I. Parvanta, Haemoglobin adjustments to define anaemia. *Trop. Med. Int. Health* **13**, 1267–1271 (2008).

49. Organisation mondiale de la Santé, *Concentrations en hémoglobine permettant de diagnostiquer l'anémie et d'en évaluer la sévérité* (World Health Organization, Geneva, Switzerland, 2011).

50. J. J. Kozich, S. L. Westcott, N. T. Baxter, S. K. Highlander, P. D. Schloss, Development of a dual-index sequencing strategy and curation pipeline for analyzing amplicon sequence data on the MiSeq Illumina sequencing platform. *Appl. Environ. Microbiol.* **79**, 5112–5120 (2013).

51. B. J. Callahan *et al.*, DADA2: High-resolution sample inference from Illumina amplicon data. *Nat. Methods* **13**, 581–583 (2016).

52. P. J. McMurdie, S. Holmes, phyloseq: An R package for reproducible interactive analysis and graphics of microbiome census data. *PLoS One* **8**, e61217 (2013).

53. P. Dixon, VEGAN, a package of R functions for community ecology. *J. Veg. Sci.* **14**, 927–930 (2009).

54. M. I. Love, W. Huber, S. Anders, Moderated estimation of fold change and dispersion for RNA-seq data with DESeq2. *Genome Biol.* **15**, 550 (2014).

55. H. Wickham, *ggplot2: Elegant Graphics for Data Analysis* (Springer, Dordrecht, the Netherlands, 2009).

56. S. Chandra *et al.*, Endoscopic jejunal biopsy culture: A simple and effective method to study jejunal microflora. *Indian J. Gastroenterol.* **29**, 226–230 (2010).

57. P. Rodriguez-Otero *et al.*, Fecal calprotectin and alpha-1 antitrypsin predict severity and response to corticosteroids in gastrointestinal graft-versus-host disease. *Blood* **119**, 5909–5917 (2012).

58. P. Vonaesch, Stunted childhood growth is associated with decompartmentalization of the gastrointestinal tract and overgrowth of oropharyngeal taxa. ENA. https://www.ebi.ac.uk/ena/browser/view/PRJEB27868?show=reads. Accessed 16 September 2022.

59. P. Vonaesch, Code related to the Afribiota project and associated publications. GitHub. https://github.com/VonaeschLabUNIL/Afribiota. Deposited 22 August 2022.